Double pulsar system J0737−3039 and its low-frequency observations with GMRT

B. C. Joshi[1*], M. A. McLaughlin[2], A. G. Lyne[2], M. Kramer[2], D. R. Lorimer[2],
R. N. Manchester[3], F. Camilo[4], M. Burgay[5], A. Possenti[5], N. D'Amico[6],
P. C. C. Freire[7]

[1]*National Centre for Radio Astrophysics (TIFR), Pune 411 007, India*
[2]*Jodrell Bank Observatory, University of Manchester, UK*
[3]*Australia Telescope National Facility, CSIRO, Epping, Australia*
[4]*Columbia Astrophysics Laboratory, Columbia University, New York, USA*
[5]*INAF-Osservatorio Astronomico di Cagliari, Capoterra, Italy*
[6]*Università degli Studi di Cagliari, Dipartimento di Fisica, Monserrato, Italy*
[7]*NAIC, Arecibo Observatory, USA*

Abstract. The recent discovery of two radio pulsars, with periods of 23 ms and 2.8 s, in a tight 2.4 hour highly relativistic double neutron star binary, is one of the most signi£cant discoveries of pulsar astronomy (Burgay et al. 2003; Lyne et al. 2004). The sharp pulses of the millisecond pulsar, the detection of its long period companion as a pulsar and an almost edge-on orbit make this system a unique laboratory for relativistic physics. The line of sight to the millisecond pulsar passes through the magnetosphere of the long period pulsar giving a unique probe of the pulsar magnetosphere. The relatively small separation between the two pulsars, a 17° per year advance in its angle of periastron and a mild eccentricity leads to a varying interaction between the pulsars, observed as a rich phenomenology in their emission. The status of research on this system since its discovery is reviewed and its low frequency observations using Giant Metrewave Radio Telescope (GMRT) are described in this paper.

Keywords : binaries: eclipsing – stars: neutron – pulsars: general – pulsars: individual: J0737−3039

---

*e-mail:bcj@ncra.tifr.res.in

1.   Introduction

The clock-like stability of the radio pulsars is their most remarkable property. Ever since the discovery of the £rst pulsar, this property has been used to measure accurately their rotation rates and their positions using pulsar timing. The presence of such clocks in a binary system is useful for a variety of reasons ranging from accurate determination of masses to detection of tiny gravitational effects as evidenced by the binary pulsar PSR B1913+16 (Hulse & Taylor 1975), and their discovery has been a major aim of all pulsar surveys in the last two decades. The discovery of two pulsars in the same binary system J0737−3039 in a high-latitude survey using the Parkes radio telescope, promises to be an exciting major discovery in pulsar astronomy (Burgay et al. 2003; Lyne et al. 2004). The double pulsar system is not only the most overdetermined double neutron star (DNS) binary discovered to date, it also exhibits rich phenomenology to probe the pulsar magnetosphere.

The two pulsars were discovered in a high-latitude survey, which used the 20 cm Parkes multibeam receiver (Staveley-Smith et al. 1996) to cover a region around the southern Galactic plane between longitudes 220° and 260° and latitudes $| b |< 60$ ° (Joshi et al. 2002). In April 2003, a 22.7 ms pulsar was discovered in a scan of this survey. The discovery plot showed a large change in the apparent pulsar period within the short 4-minute observation time indicating that this pulsar, J0737−3039A (hereafter A), was a member of a binary system. Subsequently, a 5 hour observation with the Parkes radio telescope con£rmed that the binary has a tight eccentric orbit (orbital period P_b = 2.4 hr, eccentricity $e \sim 0.09$). An improved position of the pulsar and its ¤ux density was determined using the Australia Telescope Compact Array (ATCA) via interferometric observations, which allowed the determination of orbital parameters in a short timespan. A remarkably high value of the advance of the angle of periastron, $\dot{\omega} \sim 17°$, four times that of the previously highest known value in PSR B1913+16, was measured. The measured mass function, $\dot{\omega}$ and the eccentricity of the system implied that the companion was another neutron star (Burgay et al. 2003; hereafter Paper I). This is the sixth DNS binary discovered so far (Champion et al. 2004).

No other pulsed signature was detected in the discovery observations of A, but timing data acquired subsequently showed occasional presence of 2.8 s pulsations. Further investigations revealed that the new pulsar showed Doppler variations of its apparent pulsar period, similar to A, and had the same dispersion measure (the integrated column density of free electrons along the line of sight). This suggested that the 2.8 s pulsar, J0737−3039B (hereafter B) was the unseen companion of A. The pulsed signal from B was bright in two windows of 10 min duration each and centred on orbital longitudes of 210° and 280° with respect to the ascending node, and hence was not seen in the original discovery observations, which were made at a longitude of 146°. The discovery of the companion radio pulsar in the **same** binary system opens up a unique laboratory for relativistic gravity and plasma physics (Lyne et al. 2004; hereafter Paper II). The measured parameters of the two pulsars are summarized in Paper II. The implications and the status of research about this system and its low-frequency observations with the GMRT are described in this paper.

The relevance of this discovery for tests of gravity theories is discussed in the next section, followed by a discussion of interaction of pulsed radiation of the two stars with each other in Section 3. The significance of this discovery to the gravitational wave community (Section 4) and for theories of binary evolution (Section 5) are also discussed. Finally, the low-frequency observations of these pulsars using GMRT are presented in Section 6.

2.   Experimental tests in gravitational physics

The concept of clocks has played a significant role in understanding and testing General theory of relativity (GTR). Several high-precision tests were carried out in the 1960s. Examples of such tests are the gravitational red-shift experiments involving atomic clocks (Jenkins 1969; Vessot & Levine 1979). The radio pulsar clock provides an important tool to extend these tests beyond the solar system. The neutron stars, responsible for the radio pulsations, are one of the most compact objects in astronomy distorting space-time in their vicinity considerably. The discovery of the binary pulsar PSR B1913+16 (Hulse & Taylor 1975) with its stable millisecond pulsar clock in a varying gravitational potential provided the first stringent and significant tests for theories of gravity outside the solar system (Taylor, Fowler & McCulloch 1979; Taylor & Weisberg 1989; Weisberg & Taylor 2002). The discovery of the double pulsar system PSRs J0737−3039 now not only surpasses the precision in that system, but promises to start a new era of relativity experiments.

The description of motion of stars in a compact DNS binary system requires a number of relativistic corrections to the classical Keplerian motion. These corrections were incorporated in a post-Keplerian model to investigate relativity theories soon after the discovery of the Hulse-Taylor pulsar (Damour & Taylor 1992). There are five post-Keplerian parameters (hereafter PK) in this model that have been measured in DNS binaries to date. These are the relativistic advance of angle of periastron, $\dot{\omega}$, the gravitational red-shift, γ, the orbital period decay due to gravitational radiation from the binary system, $\dot{P_b}$ and the range, r and the shape, s, of the Shapiro delay. Each of these PK parameters can be expressed as a function of the two masses (m_1 and m_2, expressed below in units of solar mass $M_\odot$) of the neutron stars in a theory of gravity. In Einstein's GTR, these relations are given by (Damour & Deruelle 1986; Taylor & Weisberg 1989; Stairs et al. 2002)

$$\dot{\omega} = 3 \left(\frac{P_b}{2\pi} \right)^{-5/3} (T_\odot M)^{2/3} (1 - e^2)^{-1} \tag{1}$$

$$\gamma = e \left(\frac{P_b}{2\pi} \right)^{1/3} T_\odot^{2/3} M^{-4/3} m_2(m_1 + 2m_2) \tag{2}$$

$$\dot{P_b} = -\frac{192\pi}{5} \left(\frac{P_b}{2\pi} \right)^{-5/3} \left(1 + \frac{73}{24}e^2 + \frac{37}{96}e^4 \right) \times (1 - e^2)^{-7/2} T_\odot^{5/3} m_1 m_2 M^{-1/3} \tag{3}$$

$$r = T_\odot \, m_2 \qquad\qquad (4)$$

$$s = x \, \left(\frac{P_b}{2\pi} \right)^{-2/3} \, T_\odot^{-1/3} \, M^{2/3} \, m_2^{-1} \qquad\qquad (5)$$

where, $M = m_1 + m_2$ is the total mass in solar units, e the eccentricity of the orbit, P_b the orbital period of the binary, $x = a_i \sin i/c$ the projected semi-major axis, $T_\odot = GM_\odot/c^3$ and c is the speed of light. Each of the above relations de£nes a curve in a $m_1 - m_2$ plot. These curves must intersect at a single point for a consistent theory. Timing the pulsar clock provides measurements of PK parameters, which can then be used to constrain the theories.

Such measurements have been possible for two DNS binaries out of the £ve known systems to date. Three PK parameters could be measured in PSR B1913+16 - $\dot{\omega}$, γ and $\dot{P_b}$ (Taylor et al. 1976; Taylor, Fowler & McCulloch 1979; Taylor & Weisberg 1982; Weisberg & Taylor 1984; Taylor & Weisberg 1989). With the two unknown neutron star masses as free parameters, the three PK parameters constrained this system, providing the £rst signi£cant test of Einstein's theory outside the solar system. A better constraint is placed by DNS binary PSR B1534+12, which has an almost edge-on orbit. This allows measurement of the delay in pulse arrival time caused by the passage of a pulse in the gravitational potential of the companion, called Shapiro delay. The measurement of Shapiro delay provides two more PK parameters in this pulsar, the range, r and the shape, s in addition to the three PK parameters measured as in PSR B1913+16. However, the observed $\dot{P_b}$ in the two pulsars is possibly contaminated by the relative acceleration of the solar system barycentre reference frame with respect to the binary centre of mass frame. The uncertainty in this correction is dominated by the uncertainty in the distance to the pulsar. Thus, even PSR B1534+12 yields four constraints to the model (Stairs et al. 2002).

Although GTR is consistent with these tests, it has been shown that there exist alternative theories which are also consistent with some £ne tuning (Damour & Taylor 1992). While $\dot{\omega}$, γ, r and s represent the strong-£eld effects, $\dot{P_b}$ is a radiative effect. In PSR B1913+16, both classes of PK parameters are required to constrain the relativity theory and hence this provides a mixed test. PSR B1534+12 provides a test for the strong-£eld effects, but an imprecise test for the radiative effects. It has been shown that theories can be constructed which satisfy such mixed tests, but differ considerably from GTR in other strong-£eld effects. For independent strong-£eld and radiative tests, a nearby nearly edge-on system with large gravitational effects, was required.

The double pulsar is just such a system. A short timing campaign at the Parkes radio telescope resulted in measurements of $\dot{\omega}$ and γ. It has an edge-on orbit as evidenced by short eclipses of A (Paper II; Kaspi et al. 2004; see section 3.1 and Figure 1) which causes Shapiro delay in its pulse arrival times. A precise measurement of the inclination angle is given by the shape parameter, $s = \sin i = 0.9995^{+4}_{-32}$, of this delay, whereas the range parameter, $r = Cm_2$ provides a constraint on the mass of the companion. These provide two strong-£eld PK parameters in addition to $\dot{\omega}$ and γ, which give a strong-£eld test of GTR in a $m_1 - m_2$ plot. The conservative estimate of its distance
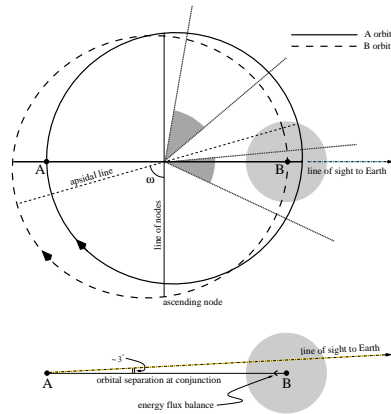
Figure 1. The physical configuration of the binary system, close to conjunction, showing the relative sizes of the two orbits and B's magnetosphere. The bottom panel shows the view of the binary from the side.

from its X-ray detection is about 1 kpc (McLaughlin et al. 2004a), although the distance indicated by its dispersion measure is about 500 pc (Paper I,II). Thus, it is a nearby system where its proper motion can be measured by parallax methods, and Very Large Baseline Interferometry (VLBI) observations to measure this are already underway. This will help in removing any kinematic effects that contaminate $\dot{P}_b$, which should be measurable in a few months' time. Thus, this system will provide an independent radiative test for theories of relativity for the first time.

The availability of two pulsar clocks for the first time provides independent estimates of projected semi-major axes of the two pulsars, x_A and x_B, permitting tests beyond what were possible with the previous DNS binaries. Their ratio ($x_B/x_A = m_A/m_B$) gives a precise measurement of the two neutron star masses independent of any theory of gravity. With four PK parameters already available, this additional constraint makes the system the most overdetermined DNS binary to date and a truly unique laboratory for relativistic gravity. These constraints have already provided one of the most accurate estimates of neutron star masses to date, 1.337 ± 0.005 $M_{\odot}$ and 1.250 ± 0.005 $M_{\odot}$, for A and B respectively. In passing, it may be noted that B has the smallest mass for a neutron star measured so far (Paper II).

Apart from classical relativistic effects, this system has the potential for tests for several tiny relativistic effects which have never been measured before. The tight orbit with two compact stars implies a substantial curvature of space-time, which influences the spin orientation of the two neutron stars causing their spin axes to precess. This will lead to pulse shape changes, similar to those observed in PSR B1913+16 (Weisberg & Taylor 2002), over a much smaller time scale of about ~ 75 years and ~ 71 years for A and B respectively (Barker & O'Connell 1975). Long-term observation of these changes potentially provide 11 pulse-structure PK parameters, at least some of which can be measured in this system with appropriate polarization observations providing new tests of gravitomagnetic effects (Damour & Taylor 1992).

The relative rapid motion of pulsars with respect to an observer on earth causes a deviation in the direction of apparent radiation known as relativistic aberration. The spin axis precession due to spin-orbit interaction causes changes in relativistic aberration which affect long-term timing of the pulsars through secular variations of eccentricity, $\dot{e}$, and of the semi-major axis, $\dot{x}$. The changes in aberration provide additional PK parameters for testing theories of gravity (Damour & Deruelle 1985, 1986; Damour & Taylor 1992).

Previous models approximated relativistic effects up to £rst-order terms, $(v/c)^2$ as the measurement errors precluded comparison with higher-order terms. However, J0737−3039 DNS binary shows an order of magnitude larger effects due to spin-orbit interaction as well as much larger $\dot{\omega}$. The strong sharp pulses of A provide higher precision timing measurements, which may soon require a revision of models to incorporate higher-order terms. The computation of Shapiro delay and modeling the bending of light in the gravitational £eld of the companion are two examples where such higher-order corrections will be useful. Lastly, the spin-orbit interaction modi£es the advance of angle of periastron, $\dot{\omega}$. An estimate of this modi£cation can, for the £rst time, provide a direct measurement of the moment of inertia of the neutron star and constrain its equation of state (Damour & Schäfer 1988; Kramer et al. 2004).

3.   Effect of interaction between A and B on their radio emission

As A rotates 44 times a second, it has a small-sized magnetosphere ($\sim$ 1200 km) bounded by its relatively small radius of light cylinder (radius of light cylinder is the distance from the neutron star where the co-rotation velocity equals the speed of light). However, B rotates 122 times slower than A. Consequently, it has a larger light cylinder (135,000 km) and a larger magnetosphere. The line of sight of the observer to any pulsar in the double pulsar passes within about 45,000 km of the other due to its edge-on orbit and the relatively small separation (900,000 km) between the two pulsars (Figure 1). As a result, the pulsed radiation of A passes through the magnetosphere of B. This leads to a rich phenomenology in the observed radiation, which is discussed in this section.

There are two major observable effects of this interaction, both of which were £rst reported in the discovery paper (Paper II). Firstly, when the line of sight to A passes through the magnetosphere of B at superior conjunction, a short eclipse of A is observed. The second effect is changes in the ¤ux density and pulse shape of B. In addition, the radiation from each pulsar appears to be modulated by the other pulsar.

3.1   Eclipses

A short eclipse of A at both 680 MHz and 1390 MHz was reported in the discovery paper (Paper II). These and subsequent Green Bank Telescope (GBT) observations have shown that the extent of the eclipse is independent of frequency of observation within measurement errors and is about 27.4 ± 1.4 s, implying that the eclipsing region has a size of 18600 km (Kaspi et al. 2004). The

eclipse has an asymmetric pro£le at all observing frequencies with a four times longer ingress than egress. The observed ¤ux density becomes zero immediately after the conjunction.

A recent reanalysis of the GBT data at 820 MHz has revealed that the pulsed ¤ux density at eclipse is strongly modulated with the periodicity of the 2.8 s pulsar. The rise and fall of ¤ux density during the eclipse is not monotonic as reported in Kaspi et al. (2004), but the pulsed ¤ux density of A is modulated with B's periodicity. This analysis separated the overall eclipse light curve into four light curves corresponding to four regions centred on B's pulse phase 0.0, 0.25, 0.5 and 0.75 respectively. The light curves corresponding to pulse phases 0.0 and 0.5 were symmetric with zero ¤ux density around the conjunction, whereas the other two light curves show a gradual decrease with zero ¤ux occurring after the conjunction (McLaughlin et al. 2004c).

The eclipse phenomenon has been explained as synchrotron absorption of A's radiation by shocked plasma which forms a cocoon around B's magnetosphere. In this model, the magnetized relativistic plasma wind of A encounters an obstacle in the form of B's magnetosphere forming a bow shock. This not only con£nes B's magnetosphere and modi£es its spin-down torque, but it also creates a magneto-sheath of relativistic hot plasma on the side of B facing A which absorbs A's radiation when the line of sight to A passes through it. Simulations of this model show that the extent of the eclipse and its mild dependence on observing frequency can be readily explained in this model by an apex cap at an appropriate stand-off distance (Arons et al. 2004; Lyutikov 2004). The pro-grade rotation of pulsar B is invoked to explain the asymmetries. The variation of pulsed ¤ux density of A with the rotational phase of B during the eclipse further supports these models (McLaughlin et al. 2004c). An explicit prediction of the model is that the eclipse will clear at frequencies higher than ∼ 5 GHz and observations have been planned to test this prediction.

If the the bow-shock model is correct, the system provides the £rst ever near probe of the pulsar wind. X-ray observations of pulsar wind nebulae (PWNe) have provided the probes for pulsar winds till recently. The ¤ow of this wind encounters an obstacle created by the circumstellar medium which is seen as PWNe. Information about the properties, such as the plasma density and the magnetization of the wind, is inferred from the radiation produced at these termination shocks. However, these provide a view of the wind far away from the pulsar which produced it. In the double pulsar, the termination shock lies much closer to the pulsar, providing a new window to study the relativistic winds. The properties of the eclipse thus provide an insight into the wind structure itself (Arons et al. 2004). Moreover, as the periastron of the system advances systematically, the variation in the eclipse phenomenon will provide a probe into the changing nature of the wind with the changing pulsar separation. Using the eclipse properties, Arons et al. (2004) have come to the conclusion that the inferred electron-positron pair injection rate is at least four times larger than the standard pair creation models, which implies a revision of these models.

3.2   Changes in average pro£le and single pulse phenomena

The interaction between A and B produces striking changes in B's pulse behaviour. Bright pulsed emission from B is seen in two windows centred on orbital longitudes 210° and 280° (Paper II). Weaker emission is also reported in two additional windows between 336° − 30° and 90° − 132° (Demorest et al. 2004). The pulse shape changes from a narrow, intense main pulse around longitude 210° to a double-peaked pulse at 280° (Paper II). A change in degree of polarization between the two bright phases has also been reported (Demorest et al. 2004). Observations at a wide range of frequencies ranging from 3030 MHz at Parkes to 336 MHz at GMRT have shown that these changes are essentially the same at all frequencies and occur at the same orbital phases with only the separation between the two components at bright phases decreasing progressively with the frequency of observations.

In addition, the 44 Hz electromagnetic radiation of A is likely to modulate the pulsed emission of B. The direct evidence for such a modulation is the recently reported detection of drifting features in B's single pulses in the orbital phase range 195° − 215°, with a ¤uctuation frequency of 0.196 cycles/period. The separation between drifting sub-pulses, P_2, is 23 ms, equal to A's period. The beat frequency between the apparent period of A as seen by B and its own period at the orbital phases where the drifting sub-pulses are seen, matches with the ¤uctuation frequency. These results imply that the drifting features are due to the impact of the 44 Hz magnetic dipole radiation of A on the magnetosphere of B (McLaughlin et al. 2004b). Thus, most of the spin-down energy is probably carried by the Poynting ¤ux of the dipole radiation instead of energetic particles as was proposed in the past (Michel 1982).

The rate of spin-down energy loss from A, estimated from the period and period derivative measurements, is 3600 times larger than that for B. Hence, the energy density of the 44 Hz radiation of A at the light cylinder of B is about two orders of magnitude greater than the radiation of B itself. This suggests that the dipole magnetic radiation / particle wind from A penetrates deep into B's magnetosphere. Assuming the standard dipole formula, this implies that the pressure balance between the energy density due to A and the magnetic £eld of B occurs at about 40 % of the light cylinder radius of B. As the two pulsars move in their orbits, the orientation of their rotation / magnetic axes will change with the orbital phase and the point of pressure balance will vary with the orbital phase, producing the observed pro£le and ¤ux density changes. In addition, the drifting features imply that the agent of interaction is the 44 Hz magnetic dipole radiation.

Another explanation for the observed pro£le and the ¤ux density variation invokes particles in A's wind and / or gamma ray radiation of A stimulating the coherent emission of B at selected orbital phases. The observed properties of A and B, such as the inner and outer angles between the two peaks of A's pro£le and similar angles between the orbital light curve of B, are £tted to non-linear relations describing the geometry of the system in this model. Such a £t provides estimates for the unknown parameters of the system, such as the orientation of the spin axis of A with respect to the orbital angular momentum vector. Assuming a precession of A's spin axis due to general relativity, the model predicts secular evolution of A's pro£le and the orbital light curve

of B (Jenet & Ransom 2004). Long-term observations of the double pulsar are required to test these predictions.

4. Implications for gravitational wave detection

The merger timescale for the double pulsar system is the shortest known (85 Myr). This, together with its low luminosity and the relative proximity compared to other known DNS binaries, implies an increase in the galactic merger rate of DNS by an order of magnitude (Paper I). Most pulsar surveys to date are biased against £nding systems similar to the double pulsar due to the large change in the apparent period of the pulsars and there may well be a selection bias against discovering such systems. After the discovery of this system, detailed simulations of the major pulsar surveys with updated population synthesis models have been carried out and the results analyzed using maximum likelihood methods. Such analysis reveals that the merger rate can be as high as 180 Myr^{-1} (Kalogera et al. 2004). This means that the terrestrial gravitational wave detectors such as LIGO and GEO could hope to detect a merger event every two years instead of once every 20 years (Paper I).

5. Origin and evolution of the DNS binary system

The double pulsar system has a tight eccentric orbit (e = 0.09) with the masses of the two pulsars being 1.337 $M_\odot$ and 1.250 $M_\odot$. This is in accord with the standard model of evolution of a DNS binary system. In these models, the more massive of the two main sequence stars evolves £rst and explodes in a supernova to form a neutron star. Under favourable conditions, it remains bound to its companion. The companion star evolves to its red giant phase gradually after which mass transfer from it to the neutron star begins with the system becoming visible as a high mass X-ray binary (HMXB). The mass transfer spins up the neutron star to millisecond periods. The unequal masses of the two stars in the HMXB cause the less massive neutron star to be dragged into the envelope of the Roche-lobe £lling companion. Since the envelope cannot be kept in co-rotation with the orbiting binary inside, a large frictional drag is generated on the binary whose orbit shrinks rapidly, eventually ejecting the envelope and forming a tight binary. The He-C-O core of the companion then undergoes a supernova leaving behind a tight eccentric DNS binary system with very different magnetic £elds and spin-down properties (Srinivasan & van den Heuvel 1982). The double pulsar is the £rst such system, where both the neutron stars have been directly detected, with exactly the same con£guration as predicted by this model.

6. Low-frequency observations with GMRT

The double pulsar system was observed at two epochs using GMRT in January and February this year to study its radio emission and other properties at low frequencies. These observations are brie¤y discussed in this section and compared with other high-frequency observations, described in the previous sections.
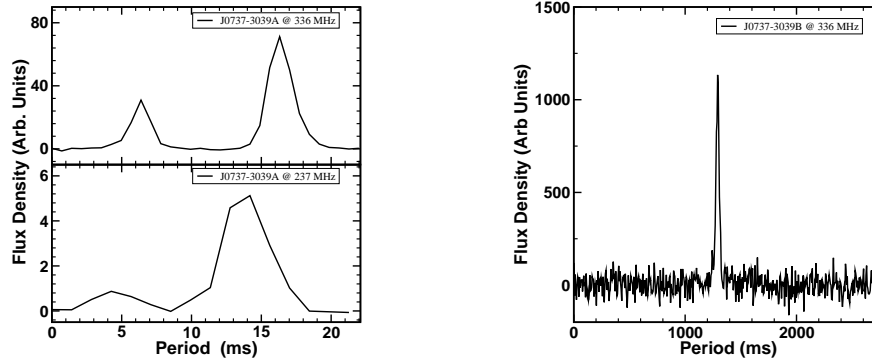
Figure 2. The integrated profiles of J0737−3039A and J0737−3039B, as observed with GMRT. (a) The left plots show the profiles for pulsar A at 336 MHz (top panel) and 237 MHz (bottom panel). The time resolution of the profile was limited by the dispersion smear and is 0.67 ms for 336 MHz and 2 ms for 237 MHz. (b) The right plot shows the profile for pulsar B at 336 MHz.

The pulsars were observed at 336 MHz with 16 MHz bandwidth using 14 central square antennas of GMRT (Swarup et al. 1991) combined in a phased array, and simultaneously at 237 MHz with 6 MHz bandwidth and using 7 of the arm antennas in an incoherently added array. The array was phased after each hour of observation to maintain a uniform sensitivity. The GMRT correlator's (Subrahmanya et al. 1995) Fast Fourier Transform Engine was used as a digital filterbank to provide 256 channels across the 16 MHz bandwidth for both the frequencies. The total power data for all channels from the phased array were recorded to hard disk at 256 μs sampling time. Similarly, the incoherent array data were recorded with a sampling time of 128 μs.

The data at both the frequencies were affected by narrowband radio frequency interference (RFI) usually observed at these frequencies. The raw data were first examined to determine the channels affected by such RFI. About 34 % of the passband was flagged as RFI at 336 MHz. The corresponding figure for the 6 MHz passband at 237 MHz was 70 %. This severely limited the sensitivity, particularly of the observations at 237 MHz where the effective bandwidth available was about 2 MHz.

The data were dedispersed and folded using the nominal DM of the two pulsars and the ephemeris given in Paper II. The dispersion smear for the 62.5 KHz width of a channel in the passband is about 0.67 ms at 336 MHz and about 2 ms at 237 MHz for both the pulsars. Hence, adjacent samples were added to keep the dispersion smear to atmost two samples for A and less than a sample for B. The data at 336 MHz were then folded to 32 bins for A and 2048 bins for B. The corresponding number of bins were 16 and 1024 respectively for the two pulsars at 237 MHz. The integrated profiles for the entire observations for the two pulsars are shown in Figure
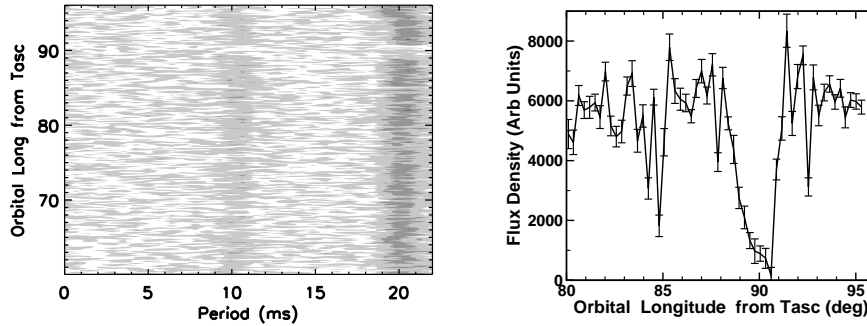
Figure 3. (a) The left plot shows the radio emission from A at 336 MHz, integrated for every 2.25 s as a function of the orbital longitude with reference to the ascending node. (b) The right plot shows the flux density (in arbitrary units) near the eclipse at 336 MHz. The time resolution of the data in this plot is 5 s.

2. Due to severe RFI flagging as well as the use of incoherent array of seven antennas, the signal to noise ratio was low in A's profile at 237 MHz and B was not detected at this frequency.

The flux density of the two components in A's profile is markedly different than at high frequencies. Whereas the two components are almost equal at 820 MHz (Ramachandran et al. 2004), the ratio of power in the two components are 2.9 and 6.6 at 336 and 237 MHz respectively. The weaker component in Figure 2 dominates the profile at 2200 MHz. The separation between the outer edges of the two features is 0.69 ± 0.09 and that between the two peaks is 0.44 ± 0.09 in units of pulse phase, and is consistent with higher-frequency observations.

To study the changes in emission with orbital phase, the data were integrated every 2.25 s for A. The short eclipse for A was detected clearly as can be seen from Figure 3a. The pulsed flux density of A was computed near the eclipse region by summing the power in the two components and is plotted as a function of the orbital phase for 336 MHz data in Figure 3b. The eclipse waveform is asymmetrical with a longer ingress timescale and a sharp egress, similar to the behaviour at high frequencies. The duration of the eclipse is about 30.0 to 35.0 s and shows no significant difference from the higher frequency observations within errors, suggesting an achromatic behaviour of the eclipse upto 336 MHz. Although A has strong single pulses, we did not have sufficient signal-to-noise ratio to study the fine structure in the eclipse waveform.

Single pulses were detected at 336 MHz in the first bright phase of B, centered at $210°$ orbital longitude from the ascending node, as shown in the Figure 4a. The structure of the pulse profile is qualitatively similar to observations at high frequencies with a two-component profile at the initial orbital longitudes evolving to a single component towards the end of the bright phase. However, the two components almost merge, unlike the clear separation at frequencies above 1 GHz. A hint of drifting features is barely visible in this figure. To investigate this further, we
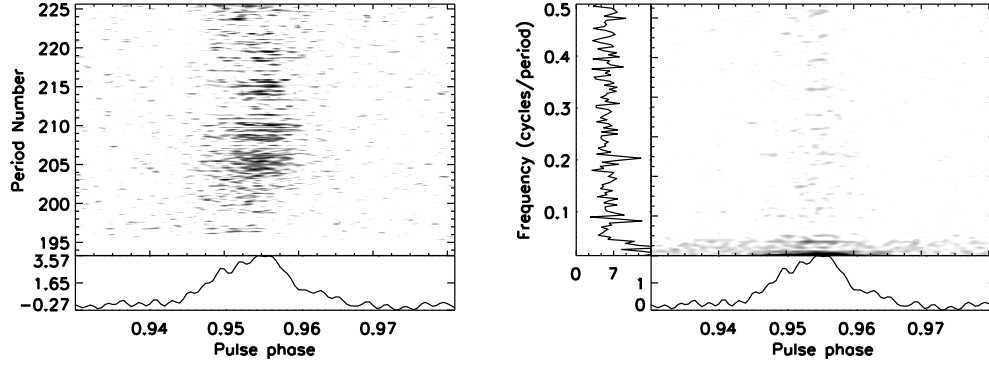
Figure 4. (a) The left plot shows the single pulses of B during the bright phase between orbital longitude 195 − 225°. The plot shows 100 bins around the pulse. The integrated profile is shown in the lower panel. (b) The right plot shows the fluctuation spectrum computed from 256 single pulses of B in the bright phase shown in the plot on the left. The bottom panel shows the integrated profile, while the phase averaged fluctuation spectrum is shown in the left panel.

computed a 256 pulse fluctuation spectrum which is shown in Figure 4b. A 3 standard deviation feature at 0.2 cycles/period is seen in this plot, which is consistent with a similar feature seen at 820 MHz with higher signal to noise ratio data (McLaughlin et al. 2004b).

The differences in the integrated profiles at low frequencies for A, although not uncharacteristic in millisecond pulsars, make future low-frequency polarization measurements important to check the consistency of polarization model for this pulsar, proposed on the basis of 820 MHz GBT observations (Demorest et al. 2004). The current geometrical model proposed by Jenet & Ransom (2004) is tentative at present and can be constrained better with such observations. The above model also makes definite predictions about the profile evolution with observation epoch, which will be tested by future observations. Similarly, the frequency and epoch dependence of B's profile in future will be useful to determine the nature of interaction between A and B, as well as constraining the overall geometry of the DNS binary.

7. Conclusions

The first one year since the discovery of the double pulsar has been very useful in setting new constraints for gravity theories and the precision of these experiments will continue to increase with time. The system exhibits rich phenomenology in its radio emission which will provide constraints for pulse emission mechanisms as well as pulsar wind models. The continuously changing viewing geometry of the system implies that the observed properties will continue to change and stimulate model making in a very unique way.

Acknowledgments

References

Arons J., Backer D. C., Spitkovsky A., Kaspi V. M., 2004, in Rasio F., Stairs I., eds, Binary Radio Pulsars. ASP Conf Series, in press (astro-ph/0404159)

Barker B. M., O'Connell R. F., 1975, *ApJ*, **199**, L25

Burgay M. et al., 2003, *Nature*, **426**, 531 (Paper I)

Champion D. J. et al., 2004, *MNRAS*, submitted (astro-ph/0403553)

Damour T., Deruelle N., 1985, *Ann. Inst. H. Poincaré (Physique Théorique)*, **43**, 107

Damour T., Deruelle N., 1986, *Ann. Inst. H. Poincaré (Physique Théorique)*, **44**, 263

Damour T., Schäfer G., 1988, *Nuovo Cim.*, **101**, 127

Damour T., Taylor J. H., 1992, *Phys. Rev. D*, **45**, 1840

Demorest P. et al., 2004, *ApJ*, submitted (astro-ph/0402025)

Hulse R. A., Taylor J. H., 1975, *ApJ*, **195**, L51

Jenet F. A., Ransom S. M., 2004, *Nature*, **428**, 919

Jenkins R. E., 1969, *AJ*, **74**, 960

Joshi B. C. et al., 2002, *Bull. Astr. Soc. India*, **30**, 687

Kalogera V. et al., 2004, *ApJ*, **601**, L179

Kaspi V. M. et al., 2004, *ApJ*, in press (astro-ph/0401614)

Kramer M. et al., 2004, in Rasio F., Stairs I., eds, Binary Radio Pulsars. ASP Conf Series, in press (astro-ph/0405179)

Lyne A. G. et al., 2004, *Science*, **303**, 1153 (Paper II)

Lyutikov M., 2004, *MNRAS*, in press (astro-ph/0403076)

McLaughlin M. A. et al., 2004a, *ApJ*, **605**, L41

McLaughlin M. A. et al., 2004b, *ApJ*, in press (astro-ph/0407265)

McLaughlin M. A. et al., 2004c, *ApJ*, submitted (astro-ph/0408297)

Michel F. C., 1982, *Reviews of Modern Physics*, **54**, 1

Ramachandran R. et al., 2004, *ApJ*, submitted (astro-ph/0404392)

Srinivasan G., van den Heuvel E. P. J., 1982, *A&A*, **108**, 143

Stairs I. H., Thorsett S. E., Taylor J. H., Wolszczan A., 2002, *ApJ*, **581**, 501

Staveley-Smith L. et al., 1996, *Proc. Astr. Soc. Aust.*, **13**, 243

Subrahmanya C. R. et al., 1995, *JA&A*, **16**, 453

Swarup G. et al., 1991, *Current Sci.*, **60(2)**, 95

Taylor J. H., Weisberg J. M., 1982, *ApJ*, **253**, 908

Taylor J. H., Weisberg J. M., 1989, *ApJ*, **345**, 434

Taylor J. H., Fowler L. A., McCulloch P. M., 1979, *Nature*, **277**, 437

Taylor J. H., Hulse R. A., Fowler L. A., Gullahorn G. E., Rankin J. M., 1976, *ApJ*, **206**, L53

Vessot R. F. C., Levine M. W., 1979, *J. Gen. Rel. and Grav.*, **10**, 181

Weisberg J. M., Taylor J. H., 1984, *Phys. Rev. Lett.*, **52**, 1348

Weisberg J. M., Taylor J. H., 2002, *ApJ*, **576**, 942